Z-scan technique to study gain properties and pump-induced processes in Ce:LiCAF UV active medium

Vadim V. Semashko*, Oleg R. Akhtyamov, Alexey A. Shavelev, Niyaz F. Rakhimov and Alexander V. Lovchev
Kazan Federal University, Kremlevskaya 18, 420008 Kazan, Russia

ABSTRACT

The preliminary data of studying optical gain properties of active media using the open aperture z-scan technique without an additional probe beam are demonstrated. The prospects of evaluating pump induced photodynamic processes parameters in UV solid-state active media on the pumping and lasing wavelengths: excited-state absorption and photoionization cross-sections of active ions, effective absorption and ionization cross-sections of color centers and recombination rates are discussed.

Keywords: z-scan, optical gain, amplified spontaneous emission, active media

1. INTRODUCTION

The combination of spectral features of ground-state absorption (GSA) cross section, gain cross section, excited state absorption cross section (ESA) and other pump-induced losses determine spectral and energy properties of active media (AM)[1-4]. That is why the measurement of these parameters is a very urgent problem. It is also important to assess the ability of the AM to amplify radiation to high power levels while maintaining stability of characteristics for a long operation time[3-7]. To evaluate these parameters the technique of pump-probe spectroscopy is usually used. Generally, pump-probe experiment requires using the high-power pumping radiation to create inverted population in the medium and probe radiation to study its response. Although the pump-probe technique is a well-developed powerful tool, it has a number of limitations. Firstly, two radiation sources with different wavelengths are needed. The first one must efficiently pump a group of given excited states while the second one must provide a radiation at the luminescence region of the sample. Secondly, to investigate the spectral and temporal dependencies of the gain a wideband or tunable source of probe beam with high spectral radiance to exceed an intensive sample's luminescence is essential. This can be achieved if an appropriate laser is used. It should be noted that pulsed lasers can cause beam's synchronization problems. At last, results of the experiments strongly depend on accuracy of spatial matching of the pumping and probing beams inside the sample. It extremely complicates the studies and is the main source of experimental errors. However, there is another opportunity to study gain properties without any external probing radiation using amplified spontaneous emission (ASE) effect[8] that requires only the pump source. This technique proposes to measure the fluorescence yield from the face of pencil-shaped AM as a function of its length and/or pumping rate. It has been successfully employed to study gain properties of gas and metal vapor lasers[9-10], organic dyes in liquid solution[11-12], semiconductors[13] and solid-state AM[14-15].

Here we propose a new technique to study gain properties of AM using the "open aperture" z-scan method[16-17]. Previously, the z-scan method was usually used for measuring non-linear features of the optically transparent sample, which was transferred through the focus of a laser beam (along the z-axis, to the sample depth direction). Because the pumping energy or the power density are changing, it also can be employed to study saturable absorption (SA) characteristics and/or ESA and non-linear photodynamic processes in AM under pumping condition[18-20]. In case of z-scanning the last ones are often exhibited as reverse saturable absorption (RSA)[21-24]. Surprisingly, to the best of our knowledge none of the researchers has taken into the account the stimulated emission (SE) as a mechanism that can affect light transmission of the sample during z-scan measurements. In this work we close this gap. The idea of a new technique is to use ASE that will cause the drop of the inversion of population and will restore the population of the ground state in AM. As a result, the absorption coefficient of the sample will depend on the cross section of the stimulated emission and pump-induced transitions, the pumping rate, and the geometry of the experiment (the spatial distribution of pump radiation into the sample). The further

*ua4pcy@mail.ru

analysis of the experimental data with various z-coordination, pumping beam energy/power allows estimating the most important AM parameters.

2. SAMPLES AND EXPERIMENT DETAILS

In order to demonstrate an ability of z-scan technique to study gain properties of the AM the Ce^{3+}: $LiCaAlF_6$ (Ce: LiCAF) wide band-gap dielectric crystal was selected as the sample. The crystal is well-known high-gain degradation-free AM for lasers and amplifiers in the UV spectral range directly pumped by the fourth harmonic of a standard Nd: YAG laser[25-28]. It operates on a four-level scheme based on vibrational-broadened allowed electro-dipole 5d-4f transitions of Ce^{3+} ions. This is why the AM has the high GSA and SE cross-sections (about ~10-17 cm^2) and corresponding saturation fluence values (~100 mJ/cm^2)[25-28], comparable with ones for organic dyes. Together with the large active ions density (~1017 cm^{-3})[19] it essentially enforces the ASE effect. Also Ce: LiCAF has the 5d-4f fluorescence quantum yield equal to 1, which leads to negligible losses of absorbed pumping energy to the heat and to the lack of noticeable pump-induced thermal distortion of the refraction index.

General problem of most solid-state UV AM based on the 5d-4f transitions of Ce^{3+} ions is the formation and accumulation of color centers (CC). The CC are formed because of the two-step $^2F_{5/2}$ (Ce^{3+}) → 5d (Ce^{3+}) → CB (6s-states of Ce^{3+} ions thermalized with conduction band (CB) of the crystal matrix) Ce^{3+} ions photoionization by pumping radiation which leads to degradation of the optical transparency and gain properties of Ce-doped solid-state materials[4]. Unlike other solid-state UV AM the Ce :LiCAF crystal demonstrates the unique high stability of laser properties for a long time of operation even at a high pumping level and/or repetition rate[28-30] and in ultrashort pulses lasing regimes[31-32]. In fact the results of many works[15,18,19,27,33] demonstrate low ESA cross-section at pumping wavelength and ESA/CC formation negligible impact on the laser properties of the Ce: LiCAF AM. It also means the lack of RSA[22].

LiCAF crystal doped with 0.5 at. % of Ce^{3+} ions in the melt had been grown by the Bridgman- Stockbarger technique in Kazan Federal University. The optical axis of the crystal was perpendicular to the growth direction. The sample has rod shape with 6 mm in diameter and 9 mm in length with uncoated polished ends.

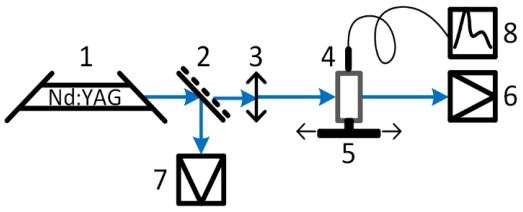

Figure 1. Open aperture Z-scan experiment setup (1 – Nd:YAG laser, 2 – fused silica wedge, 3 – 30 cm focal length lens, 4 – Ce: LiCAF crystal, 5 – linear translation stage with micrometer screw, 6, 7 – power meters, 8 – Stellarnet CCD spectrometer).

The linearly-polarized fourth-harmonic (λ=266 nm) beam from Q-switch Nd: YAG laser LS2147A from JV LOTIS TII (1) with 15 ns pulse width was used for the measurements (figure 1). The beam had a Gaussian energy distribution and it was focused on the sample (4) through the 30-cm focal length fused quartz lens (3). The lens provided the maximum pumping energy density up to 1.2-1.3 J/cm^2 in the waist with the Rayleigh's length at about 9 mm. Ce: LiCAF sample (4) was mounted on a linear translation stage (5) and was transferred through the waist of the pump radiation focusing beam with a micrometer screw. The z=0 coordinate corresponds to the focus position on the front of the crystal surface. Input and output pumping energy were controlled by double-channel Ophir optical power meter (6, 7). No apertures were used in front of power meters. Therefore the experimental set up realized the typical open aperture z-scan arrangement for the thick sample, which is specifically sensitive only to nonlinear absorption and free of any refraction index distortion[16-17]. Fluorescence of the sample was recorded with a Stellarnet CCD spectrometer (8) perpendicular to the laser beam propagation.

3. EXPERIMENTS AND DISCUSSION

Z-scan experimental results on nonlinear absorption of Ce^{3+} ions in LiCAF crystal at 266 nm wavelength are shown in figure 2. It looks unpresumable from the point of view of known phenomena, which can become apparent in the experiments. As we have already pointed above this absorption coefficient behavior with z-coordination cannot be associated neither with any pump-induced refraction index distortion, because the open-aperture z-scanning was applied,

nor neither with RSA, because the ESA cross-section is more than twice less than GSA one and no CC are detected[15,18,19,27,33].

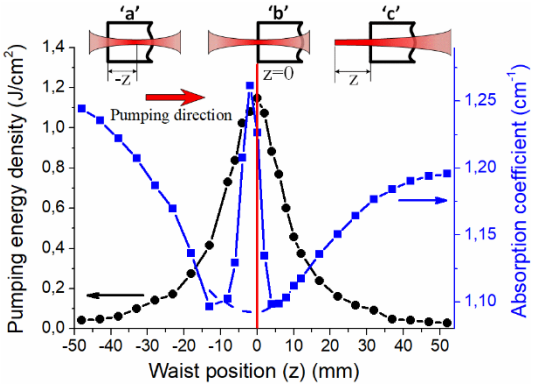

Figure 2. The pumping density (solid circles) and the Ce: LiCAF crystal absorption coefficient (solid squares) as a function of the front surface of crystal position (z-coordinate) regarding the beam's focus, the dashed line roughly shows the view of "classical" absorption saturation without considering the ASE. The waist center on the front sample surface corresponds to z=0 coordinate. Negative values of z indicate, that the beam waist is positioned inside the sample or behind him and, in contrast, positive ones mean that the focus position is situated before the sample.

The classical trends of saturation absorption are observed at relatively low pumping flux (<0.4 J/cm^2) in areas z < -20 mm and z > 15 mm roughly. However, in the area, where the pumping beam waist is located inside the sample, the trend of the absorption coefficient dependence is significantly different from the classical one and demonstrates a sharp peak at z = -2 mm. This behavior is explained by the fact that instead of the two-level medium usually considered in the theory of absorption saturation, the four-level high gain AM is studied here. In case of transferring of the pumping beam waist into the Ce: LiCAF sample the length of area with population inversion and the total gain coefficient are increased. If the length and appropriated net gain exceeds the critical ones[34], the ASE intensity drastically grows, effectively removes the inverse population between the 5d- and 4f-states of Ce^{3+} ions and, in turn, restores ground state population. Thus, the absorption coefficient of the sample again increases. Of course, it will take place when the rise time of ASE process is less than pumping pulse width, the sample has enough length and the Rayleigh's length of the pumping waist is equal or longer than critical length of area with given population inversion. For example, the ASE was revealed in Yb-doped crystals under CW and long-pulse pumping[35]. A similar effect of ASE is observed in dependence of absorption coefficient vs pump radiation density (P-scan experiments) at fixed waist positions (z-coordinate) relatively to sample's front surface (figure 3). It can be seen from the figure in case of the waist position is outside the sample (z > 2 mm or z < -8 mm) the absorption saturation curves match each other. However, when the beam waist is positioned inside the sample (-6 mm < z < 1 mm) and the pump energy density is higher than 0.3-0.4 J/cm^2, the absorption coefficient dropping rate decreases with increasing radiation intensity. Moreover, the absorption coefficient demonstrates the rise trend at z = -2 mm and energy density higher than 1 J/cm^2. This area is marked in figure 3 by a circle.

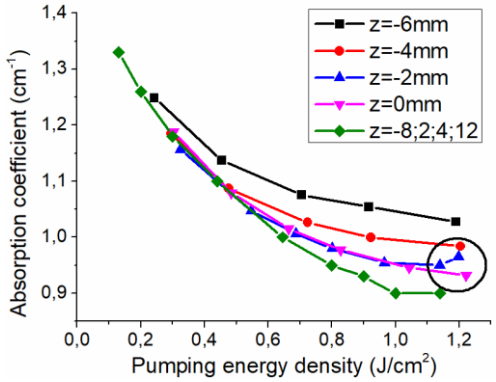

Figure 3. The absorption coefficient of Ce: LiCAF sample as a function of pump energy density (P-scan), measured at various z-coordinates

It should be noted the presence of Ce^{3+} ions multisite activation nature of LiCAF crystal, which results in the redistribution of the pumping energy between three Ce^{3+} ions activator centers[36-37]. Moreover, the lasing at about 290 nm is typically realized from only one type of Ce^{3+} centers with the largest concentration corresponding to the substitution $Ce^{3+} \rightarrow Ca^{2+}$ and non-local positive charge compensation[38]. It distorts the total fluorescence spectrum of Ce: LiCAF sample in case of laser action, because the distribution of this center's spectrum to the total one is decreased[36]. The same is observed for the sample's spectra in the z-scan measurements due to the ASE affect (figure 4) - the intensity of fluorescence of the Ce^{3+} activator center with pikes at about 290 and 310 nm is dropped and the short wavelength band's maximum shift from λ = 289.8 nm to λ = 287.3 nm at around z = -2 mm is observed.

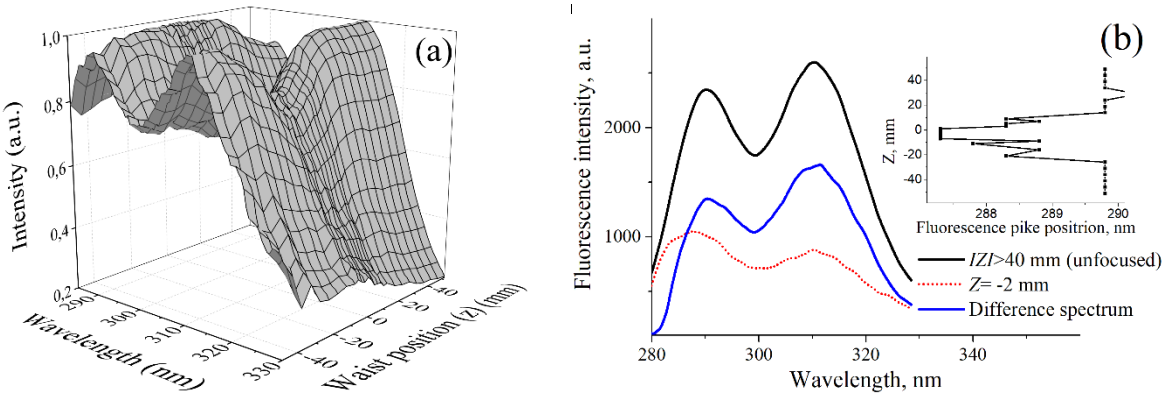

Figure 4. Typical evolution of 5d-4f luminescence spectra of Ce^{3+} ions in a LiCAF crystal versus waist position (a) and spectra for unfocussed excitation laser beam at 266 nm (z > 40), for z = -2 and their difference (b). The luminescence spectra pike's wavelength shift at around 290 nm versus the waist position (z-coordinate) is presented in the inset of (b).

The observed non-linear absorption effects were interpreted using the model of photodynamic processes in cerium-activated materials[4] (figure 5) using above-mentioned parameters determined from spectroscopic and pump-probe studies[25-27,33,35-36]. The ASE was taken into account according to the approach from the paper[39].

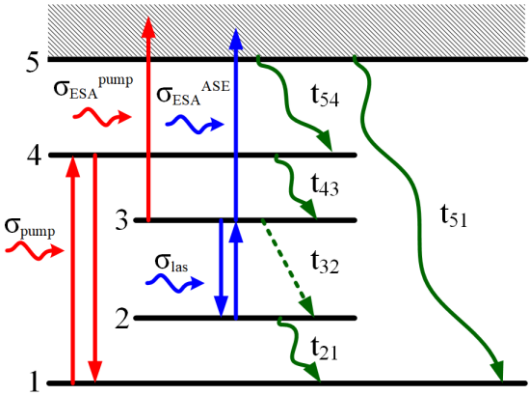

Figure 5. Stochastic model of photodynamic process in UV solid-state active media based on 5d-4f transition of Ce^{3+} ions

The model of photodynamic processes includes the conventional four-level scheme of a laser oscillator (energy levels 1-4) and the state 5 which are correspondent to conduction band of crystal host. We did not include color centers related processes in our model since we did not evidence any degradation of Ce: LiCAF crystal optical properties[33]. Direct red and blue arrows indicate light induced transitions at pump and ASE frequency, respectively. Green wavy arrows indicate nonradiative relaxation transitions and a green dotted arrow indicates radiative relaxation of the upper laser level.

The populations of each energy states and amplified spontaneous emission photon density U_{ASE} in a pulse-pumped active medium with the thickness $dz \rightarrow 0$ are determined by the appropriative balance equations (1). To take into account the relevance of contributions of different spatial areas of crystals to pumping radiation absorbance and ASE signal, this system of balance equations was sold numerically and sequentially for thin sample's layers along direction of pumping radiation propagation through the sample. The step along the time grid dt in the numerical solution of differential equations was chosen an order of magnitude less than the shortest relaxation time τ_{21} and τ_{43} and is equal to 10^{-12} sec. Partition layer

length of the sample was chosen for the calculations based on the equation $dz=c\cdot dt$, where c is the speed of light in the active medium.

$$\begin{aligned}
\frac{dn_1^i}{dt} &= -R^i(t)\sigma_{pump}\left(n_1^i - n_4^i\right) + \frac{n_2^i}{\tau_{21}} + \frac{n_5^i}{\tau_{51}} \\
\frac{dn_2^i}{dt} &= -2U_{ASE}^i(t)\sigma_{las}\left(n_2^i - n_3^i\right) - \frac{n_2^i}{\tau_{21}} + \frac{n_3^i}{\tau_{rad}} \\
\frac{dn_3^i}{dt} &= 2U_{ASE}^i(t)\sigma_{las}\left(n_2^i - n_3^i\right) + \frac{n_4^i}{\tau_{43}} - \left(\frac{1}{\tau_{rad}} + R^i(t)\sigma_{ESA}^{pump} + 2U_{ASE}^i(t)\sigma_{ESA}^{ASE}\right)n_3^i \\
\frac{dn_4^i}{dt} &= R^i(t)\sigma_{pump}\left(n_1^i - n_4^i\right) - \frac{n_4^i}{\tau_{43}} + \frac{n_5^i}{\tau_{54}} \\
\frac{dn_5^i}{dt} &= \left(R^i(t)\sigma_{ESA}^{pump} + 2U_{ASE}^i(t)\sigma_{ESA}^{ASE}\right)n_3^i - \frac{n_5^i}{\tau_{54}} - \frac{n_5^i}{\tau_{51}} \\
\frac{dU_{ASE}^i(t)}{dt} &= U_{ASE}^{i-1}(t) + U_{ASE}^i(t)c\left(\sigma_{las}\left(n_2^i - n_3^i\right) - \sigma_{ESA}^{ASE}n_3^i - K_{lum}\right) + \frac{n_3^i}{\tau_{rad}}\frac{\Omega}{4\pi}
\end{aligned}, \qquad (1)$$

where n_1^i–n_5^i are the instantaneous populations of the corresponding states for i layer. $R^i(t)$ is the pumping radiation photon flux (the time profile of the pump pulse) for i layer, where $R^1(t)$ is the pumping radiation photon flux incident on the sample, and $R^i(t)$ is equal to the one passing through the i-1 layer. σ_{pump} and σ_{ESA}^{pump} are the ground state absorption and ionization cross sections of the activator ions at the pumping radiation wavelength, respectively. σ_{las} - the cross sections of the laser transition. τ_{rad} is the lifetime of the upper laser level of active ions. τ_{ij} are the other corresponding nonradiative transition lifetimes. L is the active medium length. $U^i_{ASE}(t)$ – a flux of amplified spontaneous emission for i layer, where $U^1_{ASE}(t)=0$, whereas the ASE flux exiting layer i-1 enters layer i. Ω is the solid angle of the active medium (2):

$$\Omega = \frac{S(z)}{L^2}, \qquad (2)$$

where $S(z)$ – is the pumping laser spot area at the z - coordination.

The amplified spontaneous emission flux $U_{ASE}(t)$ for i-th thin layer can be estimated by recurrence formula (3):

$$\begin{aligned}
U_{ASE}^{\ i}(t) &= U_{ASE}^{\ i-1}(t)\cdot\exp\left[\left(\sigma_{las}\cdot\left(n_3^{i-1}(t) - n_4^{i-1}(t)\right) - \sigma_{ESA}^{las}\cdot\left(n_3^{i-1}(t) - n_5^{i-1}(t)\right)\right)\cdot dz\right] \\
U_{ASE}^{\ i=0}(t) &= 0
\end{aligned} \qquad (3)$$

The similar recurrence formula can be written for pumping energy flux after the i-th layer, which has to be used to calculation pumping rate $R_i(t)$ for the next $(i+1)$-th layer (4):

$$R^{i+1}(t) = R^i(t)\cdot\exp\left[\left(-\sigma_{pump}\cdot\left(n_1^{i-1}(t) - n_4^{i-1}(t)\right) - \sigma_{ESA}^{pump}\cdot\left(n_3^{i-1}(t) - n_5^{i-1}(t)\right)\right)\cdot dz\right] \qquad (4)$$

The absorption coefficient in the i-th layer k^i_{absorb} is (5) and their sum is the measured absorption coefficient of the sample:

$$k_{absorb}^i = \frac{1}{dz}\ln\left(\frac{\int_{-3\tau_{pump}}^{3\tau_{pump}} R_{pump}^{i-1}(t)dt}{\int_{-3\tau_{pump}}^{3\tau_{pump}} R_{pump}^{i}(t)dt}\right) \qquad (5)$$

The results of approximating the Ce: LiCAF non-linear absorption coefficient as a function of pumping waist position are shown in figure 6. Some discrepancy between the experimental and calculated curves is due to the uncertainty of the wavelength of ACE, its spectral width and divergence.

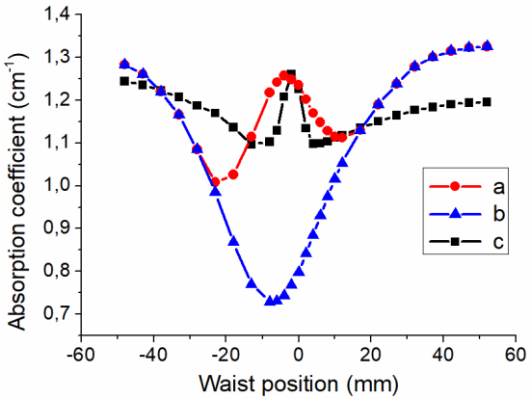

Figure 6. Approximation results of the non-linear absorption coefficient of Ce: LiCAF sample versus the pumping waist position with (a) and without (b) considering the ASE. The data (c) is the experimental one.

During the simulation, a tabulation of absorption coefficient of sample at different pump pulse duration and constant pumping rate was also carried out. As we can see from the figure 7, absorption coefficient dependence dramatically changed at pump pulse width more than 4 ns. Thus, the ASE signal arise during a time from 4 to 8 ns and can significantly affect the absorption of sample. It is that why this effect was not revealed before, because the pumping pulse width must be longer that ASE process rise-time.

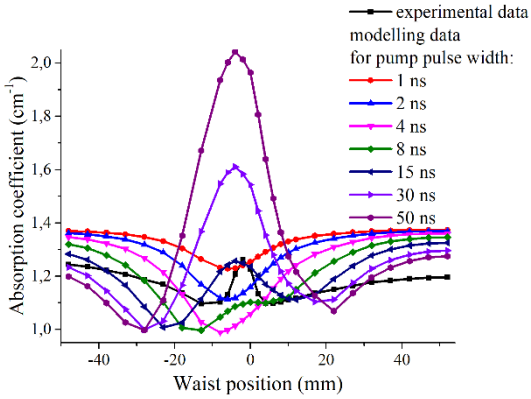

Figure 7. Tabulation of absorption coefficient of sample at different pump pulse duration and constant pumping rate

4. CONCLUSION

To the best of our knowledge the impact of ASE on the results of z-scanning experiments of thick Ce: LiCAF active media is shown for the first time. Thus, the z-scan technique can be used not only to study non-linear features of transparent samples, non-linear absorption and/or saturation effects, but also to study the gain performances.

The comprehensive studies are now in progress and the fitting procedures that will allow us to determine the basic parameters of processes in active media from z-scan experiments are being developed.

This work was supported by the subsidy allocated to KFU for the state assignment in the sphere of scientific activities [3.1156.2017/4.6] and [3.5835.2017/6.7].

The collective of authors expresses gratitude to V. A. Ostatochnikov and V. V. Pavlov for the help in mathematical modeling, which was done in the frame of Russian Scientific Foundation grant (project №15-12-10026) and grant of Russian Foundation for Basic Research [grant numbers 15-02-05309, 53/15-15].

REFERENCES

[1] Koechner, W., [Solid-State Laser Engineering], Springer-Verlag, New York (2006).
[2] Denker, B. and Shklovsky, E., [Handbook of Solid-State Lasers. Materials, Systems and Applications] Woodhead publishing series in electronic and optical materials, 35 (2013).
[3] Silfvast, W. T. [Laser Fundamentals], Cambridge university press (2004).
[4] Semashko, V. V., "Problems in searching for new solid-state UV- and VUV active media: the role of photodynamic processes," Phys. of Solid State 47(8), 1507-1511 (2005).
[5] Hamilton, D. S., "Trivalent cerium doped crystals as tunable system. Two bad apples," Hammerling, P., Budgor, A. B. and Pinto, A. eds., [Tunable Solis-State Lasers], Springer-Verlag, Berlin, 80-90 (1985).
[6] Jander, P., Sahu, J. K. and Clarkson, W. A., "High-power Er: YAG laser at 1646 nm pumped by an Er, Yb fiber laser," Proc. SPIE 5620, 297-307 (2004).
[7] Sorokin, E., "Few-cycle laser pulse generation and its applications, " Topics in Applied Physics 95, 3-73 (2004).
[8] Allen, L. and Peters, G. I., "Amplified spontaneous emission and external signal amplification in an inverted medium," Physical review A 8(4), 2031-2047 (1973).
[9] Silfvast, W. T. and Deech, J. S., "Six dB/cm Single-Pass Gain at 7229 A in Lead Vapor," Appl. Phys. Lett. 11(3), 97-99 (1967).
[10] Marowsky, G., Tittel, F. K., Wilson, W. L. and Frenkel, "Laser gain measurements by means of amplified spontaneous emission," Appl. Opt. 19(1), 138-143 (1980).
[11] Smith, P. W., Liao, P. F., Shank, C. V., Lin, C. and Maloney, P. J., "The POPOP Dye Vapor Laser," IEEE J. Quantum Electron. QE-11(2), 84-89 (1975).
[12] Shank, C. V., "Physics of Dye Lasers," Rev. Mod. Phys. 47(3), 649-657 (1975).
[13] Shaklee, K. L., Nahory, R. E. and Leheny, R. F., "Optical Gain in Semiconductors," J. Lumin. 7, 284-309 (1973).
[14] Pazzi, G. P., Baldecchi, M. G., Fabeni, P., Linari, R., Ranfagni, A., Cetica, M. and Simkin, D. J., "Optical Gain Measurements in Doped Alkali-Halides," Opt. Commun. 43(6), 405-408 (1982).
[15] Semashko, V. V., Abdulsabirov, R. Yu., Korableva, S. L., Naumov, A. K., Galjautdinov, B. M., Cefalas, A. C., Kollia, Z. and Sarantopoulou, E., "The Excited State Absorption from the 5d-States of Ce3+ Ions in LiCaAlF6 Crystals," Proceedings of SPIE 3239, 240-245 (1997).
[16] Van Stryland, E. W. and Sheik-Bahae, M., "Z-scan measurements of optical nonlinearities," Kuzyk, M. G. and Dirk, C. W. eds. [Characterization Techniques and Tabulations for Organic Nonlinear Materials], Dekker inc., Marcel, 655-692 (1998).
[17] Oliveira, L. C., Catunda, T. and Zilio, S. C., "Saturation effects in Z-scan measurements," Jpn. J. Appl. Phys. 35(5A), 2649-2652 (1996).
[18] Hai, L. H., Hung, N. D., Diwa, G., Quema, A., Marukami, H., Ono, S. and Sarukura, N., "Ce3+:LiCaAlF6 crystals as a solid-state ultraviolet saturable absorber and role of exited state absorption," Jpn. J. Appl. Phys. 44(11), 7984-7986 (2005).
[19] Galiev, A., Semashko, V., Akhtyamov, O., Shnaidman, S., Marisov, M., Nizamutdinov, A. and Shavelev, A., "Pump-probe studies of absorption saturation and optical gain in Ce:LiCaAlF6 ultraviolet active medium," J. Phys. Conf. Ser. 478, 012024 (2013).
[20] Nizamutdinov, A. S., Semashko, V. V., Naumov, A. K., Korableva, S. L., Marisov, M. A., Efimov, V. N. and Nurtdinova, L. A., "Characterization of Ce3+ and Yb3+ doped LiF-LuF3-YF3 solid solutions as new UV active media," Proc. Of SPIE 7994, 79940H1 (2001).
[21] Guliano, C. R. and Hess, L. D., "Nonlinear absorption of light: optical saturation of electronic transitions in organic molecules with high intensity laser radiation," IEEE J. Quantum Electron. QE-3(8), 358–367 (1967).
[22] Bondar, M. V., Przhonska, O. V. and Tikhonov, Y. A., "Inhomogeneous broadening of organic dyes in polymeric media: nonlinear transmission spectra and photochemical kinetics," J. Phys. Chem. 96, 10831–10837 (1992).
[23] Perry, J. W., Alvarez, D., Choong, I., Mansour, K., Marder, S. R. and Perry, K. J., "Enhanced reverse saturable absorption and optical limiting in heavy-atom-substituted phthalocyanines," Opt. Lett. 19(9), 625-627 (1994).
[24] Pritchett, T., [Models for Saturable and Reverse Saturable Absorption in Materials for Optical Limiting], Army Research Lab., Adelphi, MD, 29 (2002).
[25] Dubinskii, M. A., Semashko, V. V., Naumov, A. K., Abdulsabirov, R. Yu. and Korableva, S. L., "Spectroscopy of a new active medium of a solid-state UV laser with broadband single-pass gain," Laser Phys. 3(1), 216-217 (1993).
[26] Dubinskii, M. A., Semashko, V. V., Naumov, A. K., Abdulsabirov, R. Yu. and Korableva, S. L., "Ce3+-doped colquiriite a new concept of all-solid-state tunable ultraviolet laser," J. Mod. Opt. 40(1), 1-5 (1993).

[27] Marshall, C. D., Speth, J. A., Payne, S. A., Krupke, W. F., Quarles, G. J., Castillo, V. and Chai, B. H. T., "Ultraviolet laser emission properties of Ce 3+ doped LiSrAlF6 and LiCaAlF6", J. Opt. Soc. Am. B. 11(10), 2054-2065 (1994).
[28] Sarukura, N., Dubinskii, M. A., Liu, Z., Semashko, V. V., Naumov, A. K., Korableva, S. L., Abdulsabirov, R. Yu., Edamatsu, K., Suzuki, Y., Itoh, T. and Segawa, Y., "Ce3+ Activated Fluoride Crystals as Prospective Active Media for Widely Tunable Ultraviolet Ultrafast Lasers with direct 10-nsec Pumping," IEEE J. of Selected Topics in Quant. Electr. 1(3), 792-804 (1995).
[29] McGonigle, A. J. S., Coutts, D. W. and Webb, C. E., "530-mW 7-kHz cerium LiCAF laser pumped by the sum-frequency-mixed output of a copper-vapor laser," Opt. Lett. 24(4), 232-234 (1999).
[30] Alderighi, D., Toci, G., Vannini, M., Parisi, D., Bigotta, S. and Tonelli, M., "High efficiency UV solid state lasers based on Ce: LiCaAlF6 crystals," Appl. Phys. B. 83, 51-54 (2006).
[31] Sarukura, N., Liu, Z., Ohtake, H., Segawa, Y., Dubinskii, M. A., Semashko, V. V., Naumov, A. K., Korableva, S. L. and Abdulsabirov, R. Yu., "Ultraviolet short pulses from an all-solid-state Ce:LiCAF master-oscillator-power amplifier system," Opt. Lett. 22(13), 994-996 (1997).
[32] Sarukura, N., Liu, Z., Segawa, Y., Semashko, V. V., Naumov, A. K., Korableva, S. L., Abdulsabirov, R. Yu. and Dubinskii, M. A., "Ultraviolet subnanosecond pulse train generation from an all-solid-state Ce:LiCAF laser," J. Appl. Phys. Lett. 67(5), 602-604 (1995).
[33] Galiev, A. I., Semashko, V. V., Akhtyamov, O. R., Shnaidman, S. A., Marisov, M. A. and Shavelev, A. A., "Photodynamic processes in LiCaAlF6:Ce3+ UV active medium," J. Phys. Conf. Ser. 560, 012014 (2014).
[34] Svelto, O., [Principles of Lasers 5th eds.], Springer, Heidelberg (2010).
[35] Kazakov, B. N., Korableva, S. L., Semashko, V. V., Goriev, O. G. and Khadiev, A. R., "The experimental evidence of the amplified spontaneous emission of Yb3+ ions in LiYbF4 crystal," J. of Lum. 187, 410-413, (2017).
[36] Dubinskii, M. A., Semashko, V. V., Naumov, A. K., Abdulsabirov, R. Yu. and Korableva, S. L., "Towards the Understanding of the Physically-Limited Operation of LiCAF: Ce Tunable Solid-State Laser," OSA Proc. on Adv. Solid-State Lasers 20, 222-226 (1994).
[37] Semashko, V. V., Dubinskii, M. A., Abdulsabirov, R. Yu., Naumov, A. K., Korableva, S. L., Sherbakova, N. K. and Klimovitskii, A. E., "Investigation of Multisite Activation in LiCaAlF6: Ce3+ Single Crystal Using Stimulated Quenching of Luminescense Technique," Laser Physics 5(1), 69-72 (1995).
[38] Abdulsabirov, R. Yu., Dubinskii, M. A., Korableva, S. L., Naumov, A. K., Semashko, V. V., Stepanov, V. G. and Zhuchkov, M. S., "Crystal Growth, EPR and site-selective laser spectroscopy of Gd3+ -activated LiCaAlF6 and LiSrAlF6 single crystals," J. of Lum. 94-95, 113-117 (2001).
[39] Bogdanovich, M. V., Grigor'ev, A. V., Kabanov, V. V., Lebiadok, Y. V., Ryabtsev, G. I., Ryabtsev, A. G., Shchemelev, M. A., Dementjev, A. S., Agrawal, L. and Bhardwaj, A., "Amplified spontaneous emission induced peculiarities of the passively q-switched diode pumped erbium laser dynamics," Lith. J. Phys. 50(4), 413–418 (2010).